New Journal of Physics
The open-access journal for physics

Fast electrons from multi-electron dynamics in xenon clusters induced by inner-shell ionization

Christoph Bostedt[1], Heiko Thomas[1], Matthias Hoener[1], Thomas Möller[1], Ulf Saalmann[2,3,4], Ionuţ Georgescu[2], Christian Gnodtke[2] and Jan-Michael Rost[2,3]

[1] Technische Universität Berlin, Institut für Optik und Atomare Physik, Hardenbergstraße 36, 10623 Berlin, Germany
[2] Max-Planck-Institut für Physik komplexer Systeme, Nöthnitzer Straße 38, 01187 Dresden, Germany
[3] Max Planck Advanced Study Group at the Center for Free-Electron Laser Science, Luruper Chaussee 149, 22761 Hamburg, Germany
E-mail: us@pks.mpg.de

New Journal of Physics **12** (2010) 083004 (9pp)
Received 8 April 2010
Published 3 August 2010
Online at http://www.njp.org/
doi:10.1088/1367-2630/12/8/083004

Abstract. Fast electrons emitted from xenon clusters in strong femtosecond 90 eV pulses have been measured at the Free-electron Laser in Hamburg (FLASH). Energy absorption occurs mainly through atomic inner-shell photo-ionization. Photo-electrons are trapped in the strong Coulomb potential of the cluster ions and form a non-equilibrium plasma with supra-atomic density. Its equilibration through multiple energy-exchanging collisions within the entire cluster volume produces electrons with energies well beyond the dominant emission line of atomic xenon. Here, in contrast to traditional low-frequency laser plasma heating, the plasma gains energy from electrons delivered through massive single-photon excitation from bound states. Electron emission induced by thermalization of a non-equilibrium plasma is expected to be a general phenomenon occurring for strong atomic x-ray absorption in extended systems.

[4] Author to whom any correspondence should be addressed.

Contents

1. Introduction

The advent of high-intensity lasers in the x-ray regime brings exciting prospects such as the direct imaging of sub-nanoscale structures closer to realization [1]. It will depend critically on a detailed understanding of light–matter interaction, which is largely unexplored in this new parameter regime. Clusters, forming a bridge between the gas and the condensed phase, are an ideal tool to investigate this interaction. Indeed, exposed to intense light pulses as produced by a free-electron laser (FEL) such as the Free-electron Laser in Hamburg (FLASH) [2], rare-gas clusters have already revealed a surprising variety of phenomena, changing drastically with the photon energy. With 13 eV light, as available from the first intense short-wavelength FEL, a very strong energy absorption was found [3]. While it was immediately suspected that the absorption was due to effective inverse bremsstrahlung [4], it could be explained eventually by standard inverse bremsstrahlung of the nanoplasma in the cluster, with its ions transiently much more highly charged than suggested by the measured ion spectrum [5]. This picture of conventional plasma heating with unusually highly charged ions is supported by further experiments [6] and has proven to be beneficial as input for more macroscopic modeling of very large clusters [7]. Subsequently, almost the opposite phenomenon occurred at 40 eV light for argon; the light couples inefficiently to the cluster medium, giving rise to sequential multistep ionization with an electron spectrum differing from the atomic one merely by additional red-shifted atomic lines reflecting the gradual charging of the cluster [8, 9].

Here, we present a combined photoelectron spectroscopy and theoretical study of xenon clusters exposed to intense pulses from FLASH at 90 eV and intensities up to $I = 6 \times 10^{14}\,\mathrm{W\,cm^{-2}}$. We find exponential tails of *high-energy electrons*, which grow with higher intensities I. At a first glance the observation of such fast electrons is quite surprising for various reasons. Acceleration of electrons by the external laser field, as in the long-wavelength regime [10], cannot be efficient because of the much shorter laser period. Even acceleration through conventional heating of the trapped nanoplasma by stimulated inverse bremsstrahlung can be ruled out, as it is strongly suppressed due to its scaling of $\omega^{-8/3}$ [11] with the laser frequency ω. Moreover, high intensities I imply larger cluster charges and thus a stronger attractive potential, which rather decelerates electrons.

As we show, fast electrons originate from an equilibrated electron plasma with supra-atomic density trapped by the strong ionic Coulomb potential of the cluster. This plasma is not heated through inverse bremsstrahlung as for vacuum-ultraviolet frequencies. Rather, the plasma is 'heated' through the supply of electrons, which are released from bound states and carry excess energy after photo-absorption or intra-atomic decays. Then the trapped electrons

undergo multiple energy-exchanging collisions, where some of them acquire high velocities, which enable them to leave the cluster and to contribute to the observed high-energy tails in the photo-electron spectrum. The other electrons are slowed down and remain trapped, whereby the total energy of all electrons is redistributed but not changed.

Here, in contrast to previous studies [12], a significant fraction of ejected electrons can be even faster than those emitted from atomic xenon. This, as will be shown below, is due to the very high density of the plasma. Its formation is facilitated for 90 eV FLASH pulses in xenon by the resonant inner-shell excitation of 4d electrons with a large single-photon absorption cross section [13]. However, the formation of a dense nanoplasma, with the implication for electron emission outlined above, will occur in other systems (e.g. large molecules and systems in the condensed phase) as long as two conditions can be realized: massive atomic photo-ionization of electrons and trapping of a substantial fraction of the electrons.

2. Experimental observations

The experiments are performed at the FLASH micro focus beamline BL2 with a focal spot diameter of 26 μm full-width at half-maximum (FWHM) [14]. The FLASH x-ray pulses are 10 fs in duration and pulse energies measured pulse by pulse with a gas detector during the experimental run reach 30 μJ, leading to power densities of up to $6 \times 10^{14}\,\mathrm{W\,cm^{-2}}$ [2]. The clusters were prepared by expanding xenon gas through a 100 μm conical nozzle in front of a pulsed valve. The nozzle has been carefully calibrated previously and the cluster sizes are determined with scaling laws [15]. As the detector we use a field-free time-of-flight (TOF) electron spectrometer in which the front of the multi-channel plate detector is grounded.

Figure 1(a) displays electron distributions of xenon clusters with a mean size $\langle N \rangle = 2000$ atoms for different intensities spanning a range from below 1.0×10^{13} to $5.8 \times 10^{14}\,\mathrm{W\,cm^{-2}}$. These spectra are obtained by sorting the single-shot data into bins according to the FEL pulse energies, averaging and converting them to a kinetic energy scale. For clarity, the spectra are smoothed over 0.25 eV for energy windows below 15 eV. It should be mentioned that the sensitivity of the TOF detector is quite constant between 15 and 100 eV, but drops below 15 eV due to the decreasing detection efficiency of the multi-channel plate and the decreasing detector transmission for slow electrons. Furthermore, weakly scattered light from the clusters generates a signal that partly overlaps with the signal of very fast electrons in the TOF spectra, and therefore must be subtracted. This has been done by using the scattering signal that appears in the ion-TOF spectra of the same cluster size at the same intensity and subtracting it from the electron-TOF spectra before the time-to-energy conversion.

At the lowest investigated intensity of $1.0 \times 10^{13}\,\mathrm{W\,cm^{-2}}$, the photoelectron spectrum shows the pronounced peak of the 4d photo electrons at 20 eV and the Auger electrons around 32 eV. There is a very weak signal for faster electrons ($E \approx 40$–90 eV), which grows with the FLASH intensity and becomes most prominent at the highest value of about $5.8 \times 10^{14}\,\mathrm{W\,cm^{-2}}$. Note that this observation is opposite to former measurements with argon clusters [8], where at higher intensities, due to the larger cluster charge, slower electrons are emitted. This charging effect, which applies to photo as well as Auger electrons, seems to be superseded here by another mechanism. We focus, in the following, on this strongly power-density-dependent feature of fast electrons and present a microscopic model that explains the underlying mechanism. It reveals that fast electrons can be expected quite generally given a sufficiently high photo-ionization rate at high frequencies.

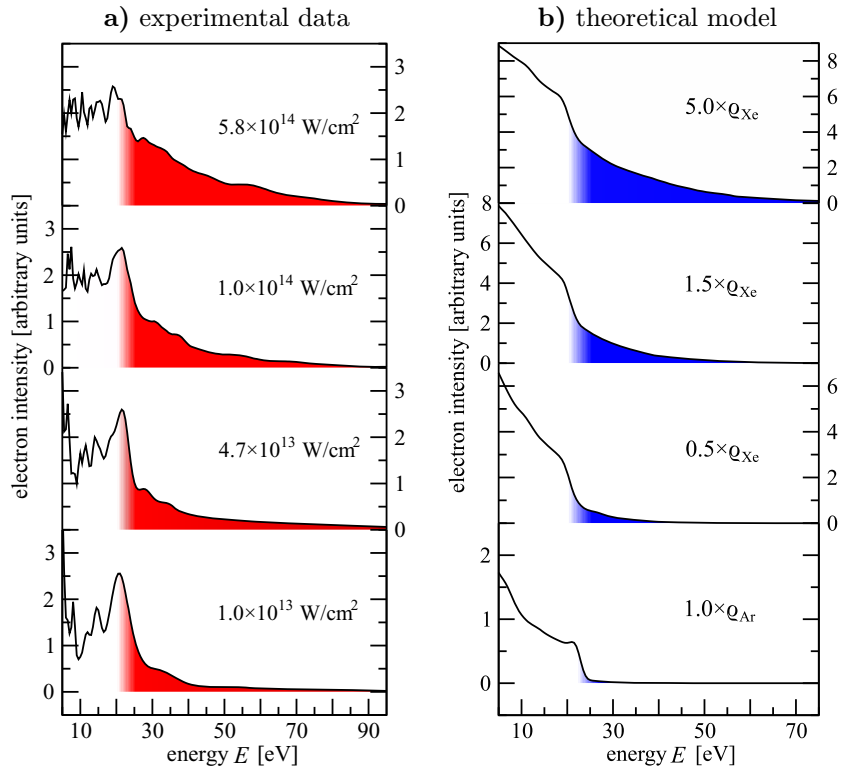

Figure 1. Electron spectra. (a) Experimental data from Xe_N clusters with $\langle N \rangle = 2000$ exposed to 10 fs FLASH pulses at 90 eV for various intensities. The red/gray-shaded areas mark electrons with energies higher than the photo peak at $E = 20$ eV. (b) Results from the simple classical multi-electron model for different electron densities (specified in the graph). The pulse duration was $T = 10$ fs for xenon (upper three spectra) and $T = 25$ fs for argon (lower spectrum). The blue/gray-shaded areas mark electrons with energies higher than the photo-peak at $E = 20$ eV (for xenon) and $E = 22$ eV (for argon).

3. Theoretical model

In order to understand the high-energy tail of the electron spectra we divide the electron dynamics of the cluster in the FLASH pulse into the initial *single photo-absorption* of bound electrons and the subsequent *multi-electron dynamics* of these electrons in the cluster potential. It is important to realize that electrons removed from an atom by photo-absorption do not necessarily leave the cluster right away. Rather, they can be trapped in the cluster potential [16], giving rise to non-trivial dynamics [17]. Hence, we call all electrons that are removed from inner-shell levels the 'activated' electrons in the following and those that are truly removed from the cluster as a whole the 'ejected' electrons. A similar division of electrons is often used in the theoretical description of laser–cluster interaction [18].

We would like to work out the general pathway to fast electrons for which the multi-electron dynamics is responsible. Therefore, we describe photo-absorption and other intra-atomic processes, like auto-ionization, only in a simplified way. The induced dynamics of interacting electrons in the ionic binding potential, however, is treated exactly by propagating

classical equations of motion. Electric fields due to a highly charged and polarizable environment easily exceed those from the laser pulse, even for a very intense pulse.

The ions are modeled as homogeneous spherical charge distribution (spherical jellium) characterized by charge Q and radius R, which also fixes the (positive) charge density of the cluster. We anticipate the total number of electrons that the light pulse is able to activate to be n. This fixes the ion charge $Q = n$, since the cluster is assumed to be charge neutral initially. The electrons are randomly distributed within the jellium sphere and are relaxed to equilibrium, from which the activation process starts. Note that the number of ions in the cluster can be smaller than Q, allowing for multiply charged ions and a supra-atomic electron density ϱ. The electrons are activated mainly in a time interval $-T < t < T$ according to a rate with Gaussian profile,

$$I(t) = I_0 \exp\left(-4 \log 2\, (t/T)^2\right), \tag{1}$$

where the length of the FEL pulse determines T. For the $n(t)$ activated electrons, we perform a classical propagation with[5]

$$n(t) = (n/2)(1 + \mathrm{erf}(2\sqrt{\log 2}\, t/T)), \tag{2}$$

obtained by integrating over the Gaussian activation rate (equation (1)) and shown as a dashed gray curve in figure 2(b). We start the calculation at $t = -3T$, where $n(t) \approx 0$ and no electron has to be propagated. At $t = 0$, where the error function in equation (2) vanishes, half of the n electrons are in motion. Note that the $n - n(t)$ not yet activated electrons stay at their initial position, but exert forces on the other electrons through the Coulomb interaction. Their inclusion is vital, since thereby all screening and charging effects, which change strongly on a femtosecond time scale due to the high xenon photo-absorption cross section (≈ 24 Mbarn), are automatically taken account of. Consequently, it is also unnecessary to adjust the ionization potentials, which are lowered or raised due to charging or screening, respectively.

Once an electron is activated by photo-absorption, it is assigned its atomic excess energy $E^\star$, in our case $E^\star = 20$ eV assuming that the electron comes dominantly from a specific shell, here the xenon 4d shell[6]. We have checked that the initialization of electrons with other energies, e.g. in order to account for Auger electrons with 32 eV, does not change the general observations and conclusions. The activated electrons are propagated under the mutual Coulomb repulsion of all other $n - 1$ electrons, as well as the attraction by the jellium potential to a time $t_{\mathrm{prop}} = 100\,\mathrm{fs} \gg T$, at which the energy spectra have converged. The laser heating at 90 eV through inverse bremsstrahlung is so small [11] that it can be safely neglected in the calculations.

4. Mechanisms of ionization

For the specific situation of the xenon cluster under the FLASH pulse at 90 eV, we have to determine the parameters (R, n, T) that enter the aforementioned electron dynamics. As is known from recent experiments under similar conditions [13, 19], xenon is highly charged by 90 eV pulses for intensities $I > 10^{14}\,\mathrm{W\,cm^{-2}}$. Atomic data at such intensities show focus-averaged charge states larger than three [19], which imply even higher charge states for atoms located at the laser axis. Since these are not known exactly, one has to rely on assumptions. We

[5] Strictly speaking, we take the nearest integer of $n(t)$.

[6] If one were to propagate only one of the electrons, the resulting spectrum would show a sharp peak at $E = E^\star$.

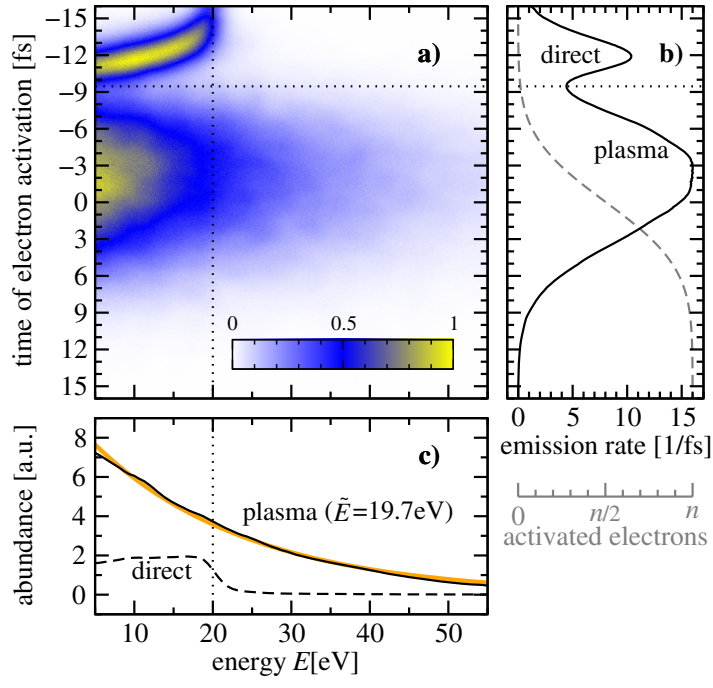

Figure 2. Time-resolved electron energy spectra. (a) Contour plot showing the final electron energy E as a function of the time when the respective electron was activated for an electron density $\varrho = 5.0\varrho_{\mathrm{Xe}}$. (b) The emission rate (black line), which is obtained by integration over the energy E. We also show the number of activated electrons (dashed gray line and gray axis), which is given by equation (2). (c) Electron spectra as obtained from the first (dashed line) and second (solid) structure in the contour plot, i.e. above and below the dotted horizontal line. The upper one can be fitted with an exponential curve (orange line) with an exponent of $\tilde{E} = 19.7\,\mathrm{eV}$.

take an average ionic charge state of five for our highest intensity of $I_0 = 5.8 \times 10^{14}\,\mathrm{W\,cm^{-2}}$. In that auto-ionization processes are implicitly taken into account. Hence, the initial electron density is $\varrho = 5\varrho_{\mathrm{Xe}}$, with ϱ_{Xe} being the atomic density of xenon. Lower intensities imply weaker photon-absorption and smaller electron numbers n. Figure 1(b) shows the results for various electron densities that are obtained for a fixed radius of $R = 31$ Å, corresponding to a xenon cluster of 2000 atoms, and $n = 10^4$, 3×10^3 and 10^3 active electrons, respectively. The spectra are obtained by averaging over 500 realizations and folding the electron energies with Gaussians of 2.3 eV width accounting for the experimental resolution. Clearly, a similar high-energy tail to that in the experimental data of figure 1(a) is visible. Moreover, it increases with larger densities ϱ. The lowest spectrum of figure 1(b) corresponds to the measurement for argon [8]. It is obtained by the model discussed above and confirms the calculations by means of a Monte Carlo simulation with perfectly sequential ionization of the cluster [8].

In order to reveal the mechanism for accelerating the electrons, we analyze the time-resolved electron spectra, as obtained from our model calculation. The abundance of electrons ejected from the cluster is shown in a contour plot in figure 2 as a function of the final energy E and the time of their activation by the absorption of a photon. Note that this time is not the time when the electron leaves the cluster, if it is temporarily trapped. One can distinguish two

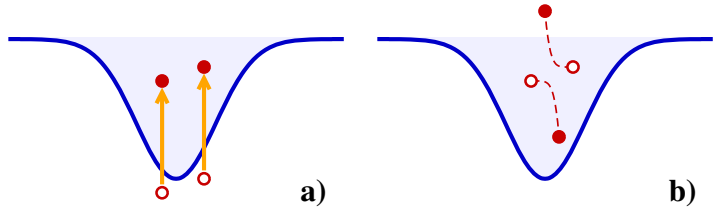

Figure 3. Schematic picture of the excitation and emission process. (a) Excitation of electrons (red points) from bound states by absorption of photons into the potential of the charged cluster (blue line). (b) Release of fast electrons from the cluster through energy-exchanging collisions. (For clarity we show only two of the many electrons that are excited and released.)

structures that are well separated in time as the integration over energy (figure 2(b)) clearly demonstrates. The first peak consists of ejected electrons activated early in the pulse and the second consists of those activated around the maximum of the pulse (near $t = 0$). As will be discussed next, the two peaks are due to *direct* and *plasma* electrons, respectively.

The emission rate of directly ejected electrons increases up to the maximum at $t \approx -12$ fs due to the increase of the laser intensity. Simultaneously, the final kinetic energy (cf figure 2(a)) is smaller for the electrons activated and ejected later on due to the increasingly deep cluster potential, an effect that has been seen before [8]. Eventually, electrons, firstly from the center of the cluster, get trapped in this potential [17]. Hence, for times $t > -12$ fs the emission rate decreases. Interestingly, however, the emission rate increases again for later times ($t > t^\star \approx -9.5$ fs, dotted horizontal line in figure 2) and—at a first glance surprisingly—particularly fast electrons are emitted.

The clear double-hump structure in figure 2(b) allows for a separation of the spectrum into two distinct parts at the specific activation time $t = t^\star$. Integrating over $t < t^\star$ and $t > t^\star$ separately results in the two spectra shown in figure 2(c). The directly ejected electrons (dashed line in figure 2(c)) only have energies below the excess energy $E^\star = 20$ eV, as observed before [8]. The step-like shape of their spectrum can be derived analytically. The second part of the spectrum (solid line in figure 2(c)) decays as $\exp(-E/\tilde{E})$ with a mean energy of $\tilde{E} = 19.7$ eV. We attribute it to the formation of a nanoplasma in the cluster, which grows due to the activation of more and more electrons. Trapped in the cluster, these electrons quickly exchange energy due to multiple collisions [20]. Thereby energetic electrons are produced that form the observed high-energy tail in the spectrum at the cost of slowing down other electrons that remain trapped. We have sketched (a) the delivery of photo-electrons into the plasma and (b) energy-exchanging collisions among the electrons in figure 3 with two electrons as an example. These are the primary processes responsible for the observed electron emission. It is instructive to study the dependence of the mean energy $\tilde{E}$ of the exponential electron distribution on the electron density ϱ. As can be seen in figure 4, $\tilde{E}(\varrho) \propto \varrho^{1/3} \propto 1/\bar{r}$, where $\bar{r}$ is a measure of the mean electron–electron distance in the cluster. Since the energy exchange through electron–electron collisions in the cluster scales with $1/\bar{r}$ the increase in figure 4 is a direct fingerprint of its relevance for the electron acceleration. This explains why a different excess energy $E^\star$, e.g. in an explicit treatment of Auger electrons, hardly changes the mean energy $\tilde{E}$.

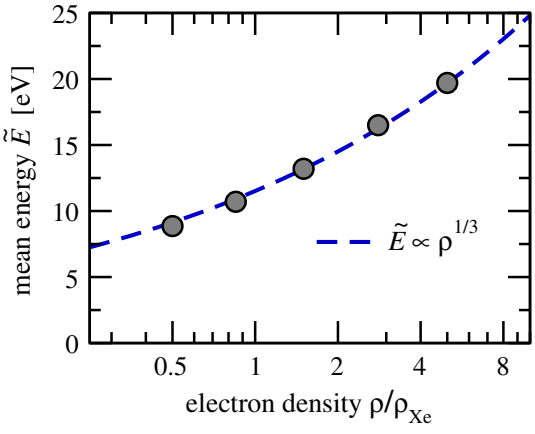

Figure 4. Mean energy $\tilde{E}$ as obtained by fitting $\exp(-E/\tilde{E})$ to electrons emitted from the plasma for various electron densities. The energies increase with the density according to $\tilde{E} \propto \varrho^{1/3}$, as shown by the dashed line.

5. Summary

Ionization of clusters in strong x-ray pulses at FLASH was measured by electron spectroscopy. The spectra of irradiated xenon clusters exhibit high-energy tails extending beyond 100 eV, which increase further with increasing intensity. We attribute their appearance to an ultrafast plasma equilibration, where the production of fast electrons occurs in energy-exchanging electron–electron collisions. Key elements are a massive single-photon ionization by an intense high-frequency pulse and the formation of a nanoplasma of high—here even supra-atomic—density trapped by the ions of the cluster. As long as these two elements are realized, this will occur in other systems, e.g. large molecules and systems in the condensed phase. Such conditions will be routinely met in operational or upcoming FEL machines operating in the hard x-ray regime, e.g. at LCLS in Stanford. There, tight beam focusing allows for peak intensities about 10^4 times larger than in our experiment. Such intensities will be essential in order to realize imaging of single molecules [1]. Thus, despite lower cross sections, multiple inner-shell ionization results in a similar plasma to that discussed here; it is transparent for the pulse, but will emit fast electrons through multiple mutual electron–electron collisions.

Acknowledgments

We thank the DESY staff for their outstanding support. Funding from the BMBF (grant no. 05KS4KTC1) and HGF Virtuelles Institut (VH-VI-302) is acknowledged.

References

[1] Gaffney K J and Chapman H N 2007 *Science* **316** 1444
[2] Ackermann W *et al* 2007 *Nat. Photon.* **1** 336
[3] Wabnitz H *et al* 2002 *Nature* **420** 482
[4] Santra R and Greene C H 2003 *Phys. Rev. Lett.* **91** 233401
[5] Siedschlag C and Rost J M 2004 *Phys. Rev. Lett.* **93** 043402

[6] Laarmann T *et al* 2004 *Phys. Rev. Lett.* **92** 143401
[7] Ziaja B *et al* 2009 *Phys. Rev. Lett.* **102** 205002
[8] Bostedt C *et al* 2008 *Phys. Rev. Lett.* **100** 133401
[9] Fukuzawa H *et al* 2009 *Phys. Rev.* A **79** 031201
[10] Saalmann U and Rost J M 2008 *Phys. Rev. Lett.* **100** 133006
[11] Krainov V P 2000 *J. Phys. B: At. Mol. Opt. Phys.* **33** 1585
[12] Ziaja B *et al* 2009 *New J. Phys.* **11** 103012
[13] Thomas H *et al* 2009 *J. Phys. B: At. Mol. Opt. Phys.* **42** 134018
[14] Tiedtke K *et al* 2009 *New J. Phys.* **11** 023029
[15] Karnbach R *et al* 1993 *Rev. Sci. Instrum.* **64** 2838
[16] Hoener M *et al* 2008 *J. Phys. B: At. Mol. Opt. Phys.* **41** 181001
[17] Gnodtke C, Saalmann U and Rost J M 2009 *Phys. Rev.* A **79** 041201
[18] Saalmann U, Siedschlag C and Rost J M 2006 *J. Phys. B: At. Mol. Opt. Phys.* **39** R39
[19] Sorokin A A *et al* 2007 *Phys. Rev. Lett.* **99** 213002
[20] Saalmann U, Georgescu I and Rost J M 2008 *New J. Phys.* **10** 025014